PROCEEDINGS OF SCIENCE

Theoretical analysis of $\Lambda(1405)$ photoproduction

Satoshi X. Nakamura*
Department of Physics, Osaka University, Toyonaka, Osaka 560-0043, Japan
E-mail: nakamura@kern.phys.sci.osaka-u.ac.jp

Daisuke Jido
Department of Physics, Tokyo Metropolitan University, Hachioji, Tokyo 192-0397, Japan

We develop a model that describes the $\gamma p \to K^+\pi\Sigma$ reaction in the $\Lambda(1405)$ region. The model consists of gauge invariant photo-production mechanisms, and the chiral unitary model that gives the rescattering amplitudes where $\Lambda(1405)$ is contained. The model also contains phenomenological parameters, associated with short-range dynamics, to be used in fitting data. We successfully fit recent CLAS data for the $\pi\Sigma$ invariant mass distributions (line-shape) in the $\gamma p \to K^+\pi\Sigma$ reaction for all the charge states. We find that the higher mass pole for $\Lambda(1405)$ of the chiral unitary model plays an important role in the reaction. We also find the nonresonant background contribution is not negligible, and its sizable effect shifts the $\Lambda(1405)$ peak position by several MeV. This work sets a starting point for a fuller analysis in which line-shape as well as K^+ angular distribution data are simultaneously analyzed for extracting $\Lambda(1405)$ pole(s).

XV International Conference on Hadron Spectroscopy-Hadron 2013
4-8 November 2013
Nara, Japan

*Speaker.

PoS(Hadron 2013)141

1. Introduction

Recently, the CLAS collaboration at Jefferson Laboratory conducted a high statistics, wide angle coverage experiment for the $\gamma p \to K^+\pi\Sigma$ reaction for center-of-mass energies $1.95 < W < 2.85$ GeV [1, 2]. In this experiment, all the three charge states of the $\pi\Sigma$ channels were simultaneously observed in the γp scattering for the first time, and the differential cross sections were measured for the $\pi\Sigma$ invariant mass distribution (line-shape) and for the K^+ angular distribution. This is the cleanest data that cover the kinematics of $\Lambda(1405)$ excitation, and it is interesting to examine if the $\Lambda(1405)$ pole(s) can be extracted from the data for the first time.

The pole structure of the $\Lambda(1405)$ resonance is a key issue to understand the nature of $\Lambda(1405)$ and the $\bar{K}N$ interaction. The coupled-channel approach based on the chiral effective theory (chiral unitary model) suggests that the $\Lambda(1405)$ resonance is composed by two poles located between the $\bar{K}N$ and $\pi\Sigma$ thresholds [3] and these states have different masses, widths and couplings to the $\bar{K}N$ and $\pi\Sigma$ channels. One pole is located at $1426 - 16i$ MeV with a dominant coupling to $\bar{K}N$, while the other is sitting at $1390 - 66i$ MeV with a strong coupling to $\pi\Sigma$ [4]. These two states are generated dynamically by the attractive interaction in the $\bar{K}N$ and $\pi\Sigma$ channels with $I = 0$ (I: total isospin) [5]. Because the $\Lambda(1405)$ resonance is composed by two states which have different weight to couple with $\bar{K}N$ and $\pi\Sigma$, the spectral shape of the $\pi\Sigma$ line-shape in the $\Lambda(1405)$ region depends on how $\Lambda(1405)$ is produced, as pointed out in Ref. [4].

It is important to confirm the two-pole structure by analyzing the new CLAS data for $\gamma p \to K^+\pi\Sigma$, and if so, it will be interesting to see how the two-pole structure plays a role in the $\pi\Sigma$ line-shape. In order to extract the $\Lambda(1405)$ resonance pole(s) from the production data, one needs to develop a model that consists of production mechanism followed by the final state interaction (FSI); $\Lambda(1405)$ is excited in the FSI. Through a careful analysis of the data, one can pin down the production mechanism as well as the scattering amplitude responsible for the FSI. Then the $\Lambda(1405)$ pole(s) will be extracted from the scattering amplitude. In this work, we consider production mechanisms that are gauge invariant at the tree-level. We consider relevant meson-exchange mechanisms, and contact terms that simulate short-range mechanisms. For the rescattering amplitude that contains $\Lambda(1405)$, we use the chiral unitary model. We successfully fit the CLAS data with it. Then we discuss a role played by each mechanism, effects of non-resonant contributions. By doing so, we set a starting point for a full analysis in which we simultaneously analyze the data for line-shape [1] and the K^+ angular distribution [2] to study the pole structure of $\Lambda(1405)$. Details of this work, including more elaborate description of the model and more results, are reported in our recent publication [6].

2. Model

We describe the $\gamma p \to K^+\pi\Sigma$ reaction by a set of tree-level mechanisms for $\gamma p \to K^+ M_j B_j$ ($M_j B_j$: a set of meson and baryon) followed by $M_j B_j \to \pi\Sigma$ rescattering, where $M_j B_j = K^- p, \bar{K}^0 n$, $\pi^0\Lambda, \pi^0\Sigma^0, \eta\Lambda, \eta\Sigma^0$, $\pi^+\Sigma^-, \pi^-\Sigma^+, K^+\Xi^-, K^0\Xi^0$, respectively. Thus the reaction amplitude for the $\gamma p \to K^+ M_j B_j$ reaction is given by $T^j = V^j + T_R^j$, where V^j is the set of tree-level photo-production mechanisms that we discuss in the next paragraph. Contribution from the rescattering is denoted by T_R^j. The rescattering amplitude is calculated with a partial wave expansion with respect to

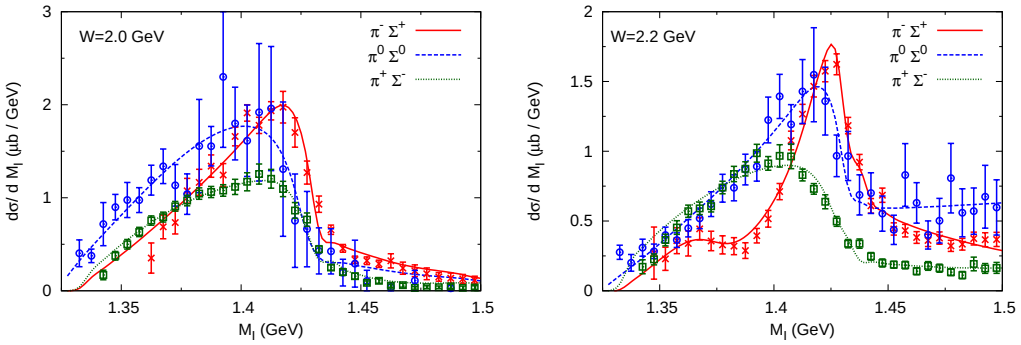

Figure 1: (Color online) Comparison of $\pi\Sigma$ line-shapes from our model with data [1] at $W = 2.0$, 2.2 GeV. Symbols for the data are cross (red) for $\pi^-\Sigma^+$, circle (blue) for $\pi^0\Sigma^0$, and square (green) for $\pi^+\Sigma^-$.

the relative motion of M_jB_j, and $(J,L) = (1/2,0)$ and $(1/2,1)$ partial waves are considered; J and L are the total and orbital angular momenta for M_jB_j. The partial wave amplitude is given, with the on-shell factorization, by $T^j_{R;JL} = \sum_{j'} T^{jj'}_{JL}\, G^{j'}\, V^{j'}_{JL}$ where $T^j_{R;JL}$ and V^j_{JL} are partial wave amplitudes of T^j_R and V^j, respectively, and are calculated with the on-shell momenta of relevant particles. For the $M_{j'}B_{j'} \to M_jB_j$ scattering amplitudes $T^{jj'}_{JL}$, we use those from the chiral unitary model given in Ref. [7] for $(J,L) = (1/2,0)$ wave, and in Ref. [8] for $(J,L) = (1/2,1)$ wave. The $(J,L) = (1/2,0)$ wave contains $\Lambda(1405)$ as double poles, while the $(J,L) = (1/2,1)$ wave provides a smooth background. We use the meson-baryon Green function, G^j, calculated with the dimensional regularization. The subtraction constants contained in G^j can depend on a channel j as well as a production mechanism contained in V^j.

We consider gauge-invariant tree-level photo-production mechanisms (V^j) as follows: minimal substitution to the lowest order chiral meson-baryon interaction such as the Weinberg-Tomozawa terms and the Born terms; vector-meson exchange mechanisms. These photo-production mechanisms are expanded in terms of $1/M_B$, and $\mathcal{O}(1)$ and $\mathcal{O}(1/M_B)$ terms are taken in our calculation.

With the meson-exchange production mechanisms and the subtraction constants taken as the same as those in the chiral unitary amplitudes, we cannot reproduce the $\pi\Sigma$ line-shape data for the $\gamma p \to K^+\pi\Sigma$ reaction from the CLAS [1]. Therefore, it is inevitable to introduce adjustable degrees of freedom to fit the data. Thus all of the meson-exchange mechanisms V^j are multiplied by a common dipole form factor, and the cutoff is fitted to the data. In addition, we also consider phenomenological contact terms that can simulate mechanisms not explicitly considered, such as, in particular, N^* and Y^* excitation mechanisms. We take couplings for the contact terms W-dependent (W : total energy of the system), and will be determined by fitting the $\gamma p \to K^+\pi\Sigma$ data [1]. The subtraction constants are also adjusted to fit the data, thereby changing the interference pattern between different production mechanisms. It is noted that we do not adjust the subtraction constants in the chiral unitary amplitudes in the fit. The subtraction constants we adjusted are all for the first loop of the rescattering, and for the renormalization of the production mechanism. By introducing quite a few fitting parameters, our method could bring a model-dependence when we extract $\Lambda(1405)$ pole(s) from the data. The model-dependence of $\Lambda(1405)$ pole(s) must be assessed by analyzing the data with different form factors and/or contact terms. This will be a future work.

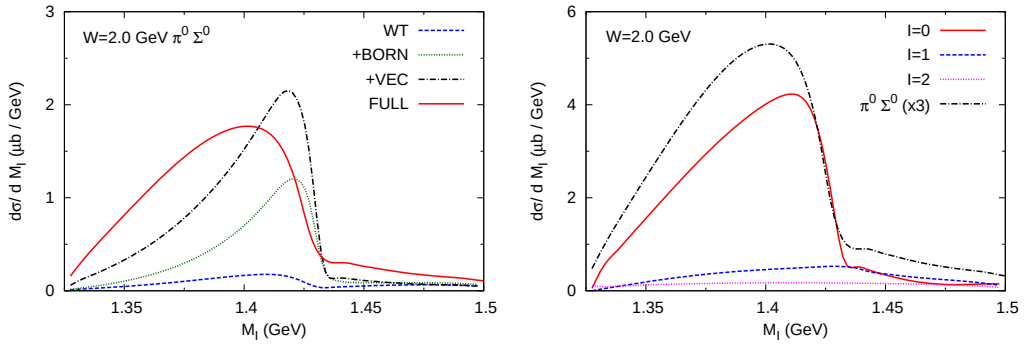

Figure 2: (Color online) (LEFT) Contribution of each production mechanism for $\gamma p \to K^+\pi^0\Sigma^0$. Contribution from the gauged Weinberg-Tomozawa terms (WT) is given by the blue dashed line. Contribution that additionally includes the gauged Born terms (+BORN) is given by the green dotted line. Contribution that further includes the vector-meson exchange (+VEC) is given by the black dash-dotted line. The full result with the contact terms is shown by the red solid line. (RIGHT) Isospin decomposition of $\pi\Sigma$ line-shapes. Contributions from the isospin states I are shown, along with the $\pi^0\Sigma^0$ line-shape multiplied by 3.

3. Result

We show the $\pi\Sigma$ line-shapes from our model in Fig. 1 where the CLAS data are also shown for comparison. Our model fits the data very well for all three different charge states of $\pi\Sigma$.

It is interesting to break down the line-shapes into contributions from different mechanisms, as shown in Fig. 2 (left). As seen in the figure, different mechanisms give significant contributions that interfere with each other. We find that the contributions from the gauged Weinberg-Tomozawa terms are rather small, as a result of a destructive interference between several gauged Weinberg-Tomozawa terms. This destructive interference is not necessarily a result of the gauge invariance, but rather relevant subtraction constants have been fixed by the fit so that the cancellation happens. Meanwhile, the contact terms, which simulate short-range dynamics, also give a large contribution to bring the theoretical calculation into agreement with the data. Finally, we mention that coupled-channels effects are mostly from the $\bar{K}N$ and $\pi\Sigma$ channels.

The difference in the line-shape between different charge states observed in Fig. 1 is a result of the interference between different isospin states. The $\pi\Sigma$ has three isospin states ($I = 0, 1, 2$), and they are separately shown in Fig. 2 (right). A dominant contribution is from the $I = 0$ state as expected due to the $\Lambda(1405)$ peak. The higher mass pole at $1426 - 16i$ MeV, that creates the prominent bump in the line-shapes, seems to play more important role than the lower mass pole. This is because the production mechanisms in our model generate $\bar{K}N$ more strongly than $\pi\Sigma$, and the final state interaction induces $\bar{K}N \to \pi\Sigma$. As shown in the previous study [4], the higher mass pole couples to the $\bar{K}N$ channel more strongly than the lower mass pole does. The $I = 1$ state gives a smaller contribution, but still plays an important role to generate the charge dependence. The $I = 2$ state contribution is even smaller, but still non-negligible. To see this point, we show in Fig. 2 (right) the $\pi^0\Sigma^0$ line-shape multiplied by 3. The difference between this and the $I = 0$ line-shape is the effect of the interference between the $I = 0$ and $I = 2$ states. We can see that the interference with the $I = 2$ state even changes slightly the peak position of the $\pi^0\Sigma^0$ line-shape.

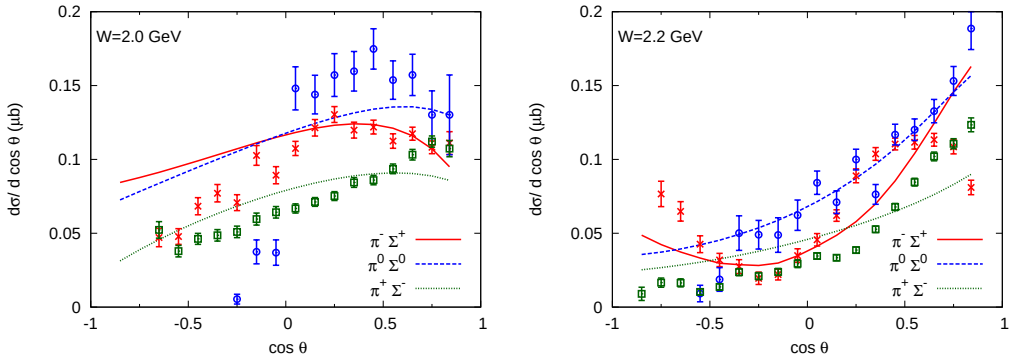

Figure 3: (Color online) Comparison of the K^+ angular distributions for $\gamma p \to K^+\pi\Sigma$ at $W = 2.0, 2.2$ GeV with data from the CLAS [2].

Fitting only the $\pi\Sigma$ line-shape data, we found several solutions whose quality of the fit to the line-shape data are comparable. However, they can have very different K^+ angular distribution. Therefore, K^+ angular distribution data will be useful information to constrain the production mechanism. Recently the CLAS Collaboration reported data for the K^+ angular distributions [2]. Here we show in Fig. 3 the K^+ angular distributions from our model that reproduces the data relatively better than the other solutions. At $W = 2.2$ GeV, our model captures overall trend of the data. However, for the $\gamma p \to K^+\pi^0\Sigma^0$ reaction at $W = 2.0$ GeV, there is a sharp rise in the data at $\cos\theta \sim 0$ while rather smooth behavior is found in the calculated counterpart. We actually tried fitting the K^+ angular distributions data, but this sharply rising behavior cannot be fitted with the current setup. It seems that we need to search for a mechanism that is responsible for this behavior. We leave such a more detailed analysis of the K^+ angular distribution to a future work.

Acknowledgments

SXN is the Yukawa Fellow and his work is supported in part by Yukawa Memorial Foundation. This work was partially supported by the Grants-in-Aid for Scientific Research (No. 24105706).

References

[1] K. Moriya *et al.* [CLAS Collaboration], *Phys. Rev.* C **87**, (2013) 035206.

[2] K. Moriya *et al.* [CLAS Collaboration], *Phys. Rev.* C **88** (2013) 045201.

[3] As a recent review on the application of the chiral unitary approach to Λ(1405), T. Hyodo and D. Jido, *Prog. Part. Nucl. Phys.* **67** (2012) 55.

[4] D. Jido, J. A. Oller, E. Oset, A. Ramos and U. G. Meissner, *Nucl. Phys.* A **725** (2003) 181.

[5] T. Hyodo and W. Weise, *Phys. Rev.* **C77** (2008) 035204.

[6] S.X. Nakamura and D. Jido, Prog. Theor. Exp. Phys. (to be published); arXiv:1310.5768 [nucl-th].

[7] E. Oset, A. Ramos, and C. Bennhold, *Phys. Lett.* B**527** (2002) 99.

[8] D. Jido, E. Oset, and A. Ramos, *Phys. Rev.* C **66** (2002) 055203.